Digest Journal of Nanomaterials and Biostructures Vol. 17, No. 4, October-December 2022, p. 1181-1190

Investigation of the physical properties and Mulliken charge distribution of the cube perovskite $BiGaO_3$ is calculated by GGA-PBE

A. M.Ghaleb[a,*], A. Th.Shihatha[b], Z. T.Ghaleb[c]
[a]*Department of Physics, College of Science, University of Kirkuk/Iraq*
[b]*Ministry of Education , Kirkuk Education Directorate/Iraq*
[c]*Department of Chemistry, College of Science, Kirkuk University, Kirkuk/Iraq*

We systematically studied the structure, electronic, elastic and optical properties of $BiGaO_3$ type perovskite cubes. We also report the calculation of all properties listed in the title of GGA-PBE approximation to $BiGaO_3$.This material has a band gap which can be considered as an indirect band gap. The maximum valence band is represented by the M point (VBM), whereas the conduction band is represented by the X point (CBM)The electronic structure of BiGaO3 shows that it has a semiconductor indirect band gap of 1.37 eV.The elastic constant was determined in equilibrium confirming its accuracy. The bulk, shear, and Young's modulus were all extracted from the data. Poisson's ratio was also found. The confirmed structural parameters were in good agreement with the previously calculated experimental data. Our research suggests that $BiGaO_3$ is a promising piezoelectric, multiferroic, ferroelectric, and photo catalytic material.

(Received June 7, 2022; Accepted October 13, 2022)

Keywords:$BiGaO_3$, GGA approximation, Optical properties, Elastic constants, Electronic properties.

1. Introduction

Various composite oxides were extensively studied. However, perovskite oxide is especially versatile, showing anextent of different applications. Studies on this topic have been ongoing for quite some time now [1].Recent studies have shown that perovskites, which include materials with Bi-metal transitions, have a lot of potential for various applications. [2]. Perovskite oxides are gaining more attention due to their technical applications such as electronic devices, light waves, piezoelectricity and iron [3-5].A group of materials commonly used for lead-based iron and piezoelectric devices (such as $PbTiO_3$ and $PbZrO_3$). Due to the toxicity of lead, it was necessary to find materials that have similar properties and do not pollute the environment. Several attempts have been made in recent years for a solid $BiGaO_3$-based solution. Bi-based oxide compounds containing the non-magnetic element Ga have been receiving much attention due to the materials solid solution can enhance the photoelectric features of lead titanate and reduce the lead content[6].Bismuth gallate $BiGaO_3$ was produced experimentally using high-pressure and high-temperature technologies[7].Investigations on the physical properties of bulk and nanostructures of these compounds are limited, when compared to other multi-ferroic materials. Theoretically, the piezoelectricity and large ferroelectric polarization of $BiGaO_3$ were predicted [4,8,9].Using the basic principles of density functional theory calculations to determine the electronic properties, structure and instability of the four cubic perovskites $BiMO_3$ with M (M = Ga, Al, In and Sc). A research has shown that $BiMO_3$ oxides or modified versions are promising photo catalysts, ferroelectric materials, piezoelectric materials, and multiferroic materials[10,11].In this study, we focused on the physical properties of $BiGaO_3$ using density functional theory. This is important because it allows us to understand the compound completely, which is necessary for its use in technological applications. Elastic constants provide valuable information about the anisotropic character of the bonding and structural stability.

* Corresponding author: abdlhadig4@gmail.com
https://doi.org/10.15251/DJNB.2022.174.1181

2. Method of calculations

It is assumed that the considered $BiGaO_3$ has an ideal cubic perovskite structure with space group Pm3m (#221). Here, the atomic positions of the primitive units are represented by Bi:1a(0,0,0), Ga:1b(0.5,0.5,0.5) and O:3d(0.5,0,0) are defined. The electronic configuration of the compound is assumed to be $4f^{14}5d^{10}6s^26p^3$, $3d^{10}4s^24p^1$, $2s^22p^2$ for Bi, Ga and O respectively.The Kohn-Sham density functional theory is a well-known and reliable method for simulating the ground state characteristics of atoms, molecules, and solids. This theory can be accurate without knowing the exact form of the electron density; because many-body problems are complex and nonlinear, approximations are made to make the theory tractable[12].A generalized gradient approximation is one of the most popular functional approximations (GGA)[13].The GGA are now ready, and they contain PBE[14].The Broyden–Fletcher–Goldfarb–Shanno minimization method was used for structural optimization (BFGS)),the force on each ion converged to less than 0.01eV/ A°.A cut-off of the kinetic energy of (800) eV and a total energy convergence threshold of (1×10^{-6}) eV were used. The Brillouin zone integrations were performed by using a Γ-centered ($12 \times 12 \times 12$) k-point grid.

3.Results and discussion

3.1. Geometry optimization and Band structure

The $BiGaO_3$ compound crystallizes in the Pm3m(#221) space group, which is ideal for cubic perovskites. (5 atoms) per unit cell. Figure (1) shows the crystal structure of $BiGaO_3$ at room temperature. It can be noticed that Bi cation appears at the corner of the cube, with the oxygen ion in the center of the plane in the center cation. This indicates that $BiGaO_3$ has achieved a cubic structure. The structural parameters of the $BiGaO_3$ cube have been calculated. The results are summarized in Table (1) which shows that the lattice constant (a) is overestimated by about 0.5%. These deviations are within the permissible range of first-principles error. Our findings are similar to these of other researchers who have used the full potential linearized augmented plane wave (FP-LAPW) method[10,11].Table (1) includes these values as well as other theoretical results.

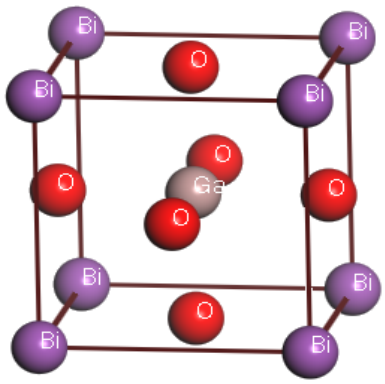

Fig. 1. Cube lattice structure of $BiGaO_3$.

Table 1. Calculated equilibrium lattice parameters, volume and band gap for $BiGaO_3$ compound in comparison with the available theoretical results.

Parameter	$a(A^\circ)$	$V(A^\circ)^3$	Eg (eV)
this work	3.8573	57.389	1.37
[10] [11]	3.905 3.816	59.547 55.568	1.34 1.41

Figure (2) describes the energy band gap of $BiGaO_3$.The GGA-PBE technique is a powerful way to determine the band structure along the high symmetry Γ, R, M direction of, and the Brillouin zone represented in X. $BiGaO_3$ compound has an indirect energy band gap (1.37 eV).Figure (2) Shows that the CBM and VBM are located at points that are completely different from each other. points M (k = 2π / a (110)). and X in the Brilloun zone (k = 2π / a (100)). Our indirect band gap (MX) calculation is consistent with the values of the other calculations listed in Table (1).

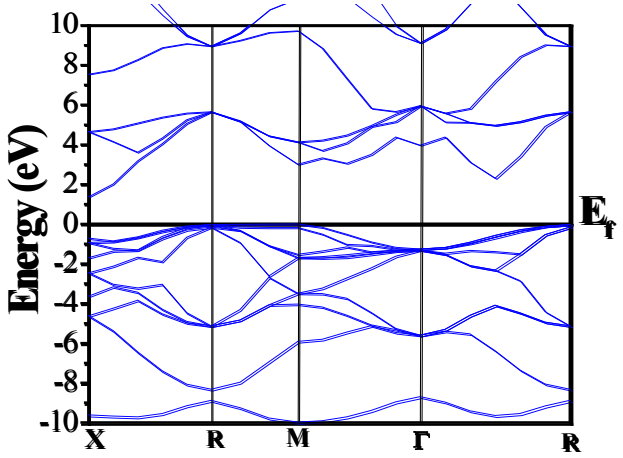

Fig. 2.The energy band structure of a $BiGaO_3$ compound has been calculated.

3.2. Density of states (DOS)

To clarify the nature of the electronic band structures of $BiGaO_3$, the total density (TDOS) and partial density of states (PDOS) were calculated. It is shown in figure (3) that PDOS can determine the nature of the angular momentum of various structures. From figure (3), the valence bands VB can be divided into four different energetic regions. The first region of the energy spectrum extending from -22.8 to -22 eV which includes Bi-5d. The second region starts from a energy range of -8.5 to -18.7 eV, which is dominated by the O-2 state that has a small contribution to the state of Ga-3d.A third region from -14.7 to -12.4 eV. consisted of Ga-3d orbital states. Finally, it is clear that dominating states of O-2p are in the range of 0 and -6.6 eV (upper VB), with a mixture of Ga-sp and Bi-6P orbitals.The hybridization of Ga atoms and O atoms in this region is located near the Fermi level indicates that the Ga-O bond is a covalent bond. The lower part of the band gap of $BiGaO_3$ is mostly filled by the 6p state of Bi, while the upper part is mostly filled by the s and p states of Ga. The s and p electrons of Ga force the Bi-6p state closer to the Fermi level. Our calculations of the band structure, TDOS and PDOS of $BiGaO_3$ are consistent with previous theoretical results[10,11].

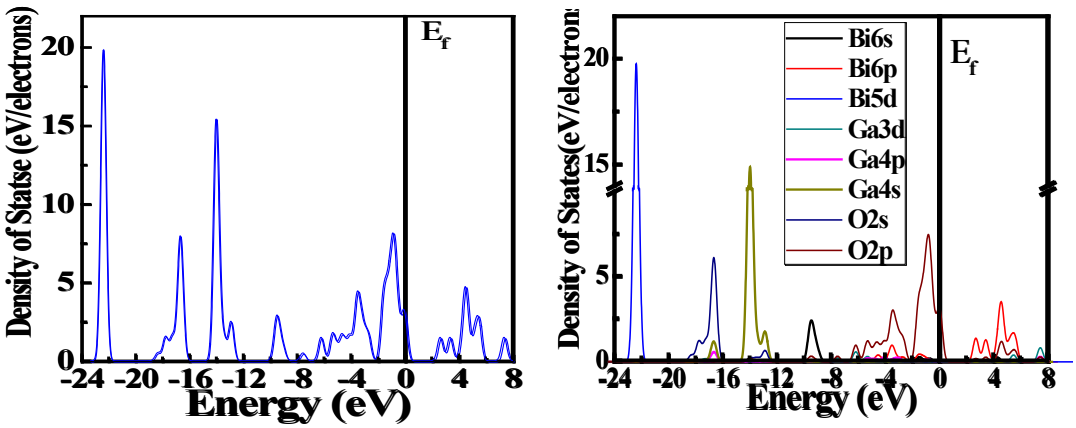

Fig. 3. Calculated total density of states (TDOS) and partial density of states (PDOS) of $BiGaO_3$ at the predicted equilibrium lattice constant.

We have also used the Mulliken charge collection of $BiGaO_3$ to describe the behavior of bonds. Table (2) shows the Mulliken population charge values. Due to the transferred charge from Bi to O is approximately 1.51 electrons and the transfer of the charge from Ga to O is 1.29 electrons, we deduced that $BiGaO_3$ bonding characteristic is a mix of ionic and covalent nature. Furthermore, the bond between Ga-O is a covalent bond that is highly strong, which stronger than the bond between Bi-O.

Table 2.Mulliken charge population of cubic perovskite$BiGaO_3$.

Species	s	p	d	f	Total	Charge (electron)
O(1)	1.86	5.07	0.00	0.00	6.93	-0.93
O(2)	1.86	5.07	0.00	0.00	6.93	-0.93
O(3)	1.86	5.07	0.00	0.00	6.93	-0.93
Ga(1)	0.61	1.11	10.00	0.00	11.71	1.29
Bi(1)	2.00	1.48	0.00	0.00	3.45	1.51

3.3. Optical properties

Figure (4) depicts the estimated optical characteristics at the equilibrium lattice constant for energy ranges up to 30 eV. In order to calculate the observed structures in the spectrum, one must consider the transition between occupied and unoccupied energy bands in the structure of the electronic energy bands at high symmetry points in the Brillouin zone and must be considered According to the explanation[15]. The dielectric properties are expressed by using the Kramer–Krung relationship for the complex dielectric function$\varepsilon(\omega) = \varepsilon_1(\omega) + i\varepsilon_2(\omega)$ [16].The first part, $\varepsilon_1(\omega)$ is the real part, which determines the polarization and scattering of light, and the second part, $\varepsilon_2(\omega)$ is the imaginary part that describes the absorbance of the material. The real part of dielectric function $\varepsilon_1(\omega)$ is shown in Figure (4(a)) in the energy range (0-15)eV. The static value of $\varepsilon_1(0)$ is (5.7) is observed for $BiGaO_3$, $\varepsilon_1(\omega)$ continues to increase from $\varepsilon_1(0)$, reaching the value at maximum level before decreasing below zero at specific ranges of energy. The incident photon beam at these energy bands is completely weakened where a negative value in this region means a loss in energy transmission as well as a weakening in light transmission. Based on the $\varepsilon_2(\omega)$ spectra in Figure 4(a), it is clear that the first critical points for $BiGaO_3$ occur at about 2.75eV. This agrees with our predictions. The fundamental absorption edges [17] are caused by the direct inter-band transitions VBM and CBM in the $BiGaO_3$ compound. Electrons travelling from Oat the 2p states in the valence band region to the Ga at the4s states in the conduction band

region after (2.9 and 4.6)eV. Our calculated optical and electronic properties suggest that the investigated compounds are possible to be implemented in photovoltaic cell fabrication, according to practical studies[18].The extinction index and refractive index are found to help analyze the degree of transparency of the studied material and the ability of absorbing incident light (photons).The relation of extinction coefficient $k(\omega)$ and refractive index $n(\omega)$ with real part are as follows:

$$k(\omega) = \sqrt{\frac{|\varepsilon(\omega)| - \varepsilon_1(\omega)}{2}} \quad (1)$$

$$n(\omega) = \sqrt{\frac{|\varepsilon(\omega)| - \varepsilon_1(\omega)}{2}} \quad (2)$$

Figure 4b shows the refractive index n(ω) and extinction coefficient k(ω) of $BiGaO_3$. Over the wide-range energy over 15eV, the values of refractive index spectrum of n(ω) is very broad. n(ω) and $\varepsilon_1(\omega)$ seem to have the same character. It can be shown in Figure 4b that n(ω) increases as the energy peaks at 4.45 eV for $BiGaO_3$.The ultraviolet is represented by a peak in the transparency region, which then descends to a minimum level at 7.5eV. $BiGaO_3$'s static refractive index n(0) varies inversely with the band gap, with calculated values of approximately 2.44.Fig. (4d) shows that extinction coefficient k(ω) local peaks correspond the static component of $\varepsilon_1(0)$.The final behavior of the k(ω) and n(ω) peaks is determined to be similar for the compound and in good agreement with another anticipated investigation of the k(ω) and n(ω) peaks [19].The wavelength-dependent reflectance coefficient R(ω) for $BiGaO_3$ is shown in Figure (4c). R(0) is the static reflectivity. The first peak is at 3.4eV.It is worth noting that the reflectivity achieves a maximum when $\varepsilon_1(0)$ is smaller than zero. The material shows the metallic characteristic for negative values of $\varepsilon_1(\omega)$[20].Because a compound's reflectivity is proportional to its metallicity, its value R(0) is greatest for negative $\varepsilon_1(\omega)$As shown below [21], the absorption coefficients α(ω) reflect the influence and efficiency of any material in absorbing energy packets (photons) with respect to photons of light of energy E=hw.

$$\alpha(\omega) = \sqrt{2}\omega\left[\sqrt{\varepsilon_1^2(\omega) - \varepsilon_2^2(\omega)} - \varepsilon_1(\omega)\right]^{\frac{1}{2}} \quad (3)$$

The $BiGaO_3$ absorption coefficients α(ω) of are shown in Fig (4d). The significant absorption zones of the examined materials are supported by comparing with Figure (4a) $\varepsilon_1(\omega)$, $BiGaO_3$ should be optically active in these locations. According to the computed data, the absorption coefficient for $BiGaO_3$ exhibits a sharp edge about 16 eV. These sharp absorption coefficients edges are similar to the band gap of semi-conductive materials, which allow only photons with sufficient energy to stimulate an electron to the unoccupied levels of the conduction band from the occupied levels of the valence band to be seen into the material. The presence of high absorption zones of 12-17eV perovskite, may indicate that they are promising candidates for optoelectronic device applications in the UV range. The observed optical conductivity Fig. (5e), Applying energy will result in a response in optical conduction after 2.35eV for $BiGaO_3$ respectively. The $BiGaO_3$ optimum optical conductivity is approximately at 5.6eV. The $L(\omega)$ spectra of $BiGaO_3$ are shown in figure (4f), it is obtained that the maximum peak is located at 22 eV. The electron energy loss function $L(\omega)$ plays an important role in describing the energy lost for a fast electron passing through a material. The prominent peaks in the $L(\omega)$ spectra represent the property associated with plasma resonance (mass oscillation of valence electrons) and the corresponding frequency is the so-called plasma frequency $\omega(p)$ [22].The peaks of $L(\omega)$correspond to the trailing edges in the reflection spectra, where the occurrence of prominent peaks of $L(\omega)$figure (4f) can be observed at energies corresponding to the abrupt reductions of $R(\omega)$ figure (4c).The function for calculating electron energy loss L(ω) is used to describe the energy lost by a rapid electron traveling through a materials. The large peaks in the L(ω) spectra

show the plasma resonance property (mass oscillation of valence electrons), and the related frequency is known as plasma frequency ω(p) [22].

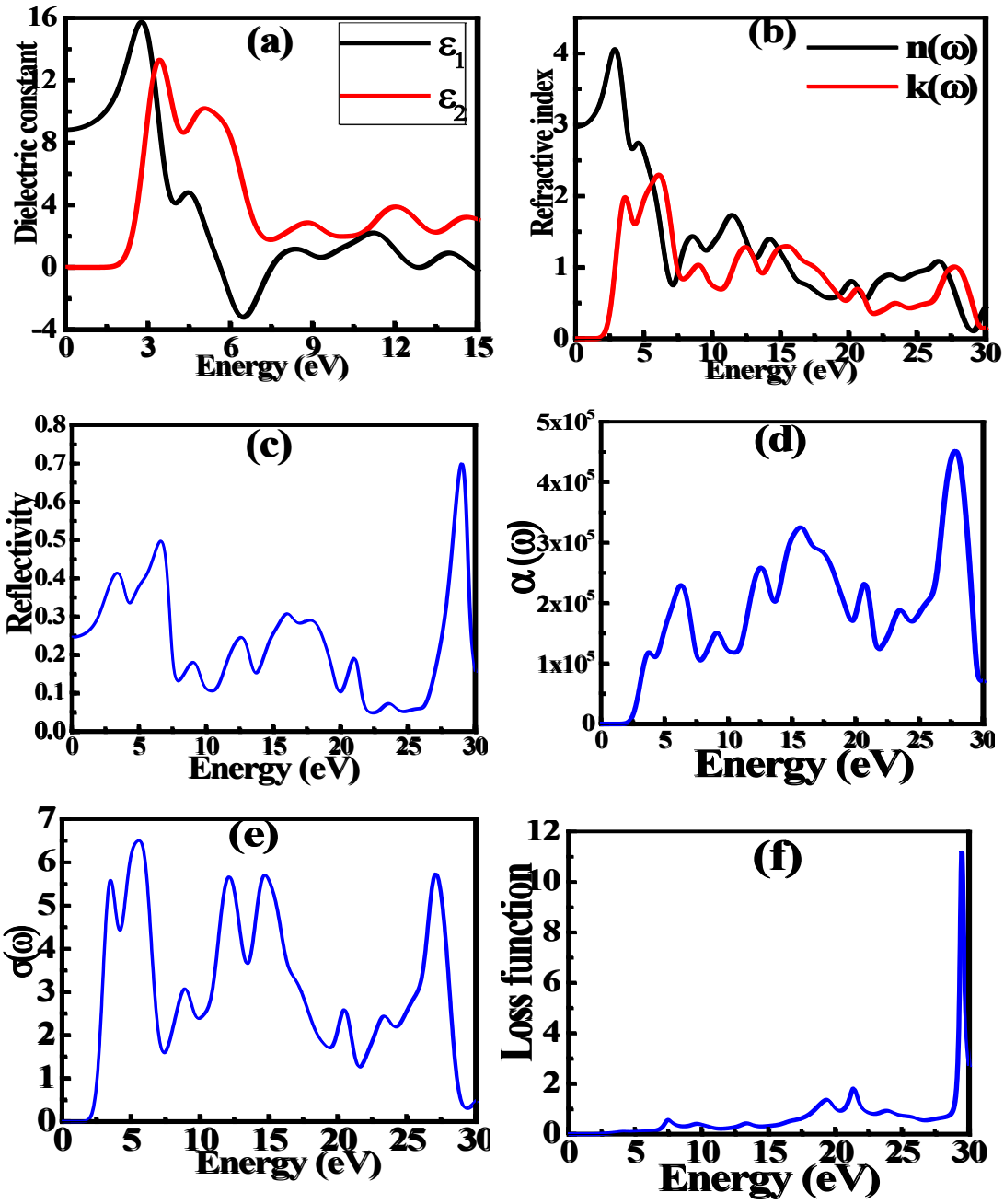

Fig. 4. Calculated optical constants for $BiGaO_3$:dielectric function:(a) real part $\varepsilon_1(\omega)$and imaginary part $\varepsilon_2(\omega)$(b)The extinction index $K(\omega)$ and the refractive index $n(\omega)$,(c)The reflectivity $R(\omega)$,(d)the absorption coefficients $\alpha(\omega)$,(e)The photoconductivity σ (ω), and (f)loss function $L(\omega)$.

3.4. Elastic properties

The elastic constants, which play a key role in supplying valuable information on the correlation property between neighboring atomic levels, determine the qualities of a material that endures deformation and stresses and restores its original shape after the stress is removed. In general, the importance of the elastic constants of solids lies in the fact that they provide a link Between the mechanical and dynamic behavior of crystals. Table 3 shows the elastic moduli of $BiGaO_3$ calculated using the perturbation method at equilibrium pressure within the GGA-PBE

approximation . In this table we present the calculated values of the elastic constants C_{ij}.The cubic system is characterized by three different symmetry elements ($C_{11}, C_{22},$ and C_{44}),in cubic crystals, the elastic contrast factor (A) is a measure of the solids elastic anisotropy degree, defined as $A = 2C_{44}/(C_{11} - C_{12})$,the material is completely isotropic If the value of $A = 1$. If A value of is less or greater than 1 it means that the value of elastic anisotropy degree is shown. Our calculations showed Zener anisotropy for $BiGaO_3$ is less than 1, indicating that $BiGaO_3$ is an anisotropic material, according to what the researchers also explained [23]. Moreover, Bulk modulus B is a linear combination of elastic constants (C_{11} and C_{12}) for cubic systems. Where C_{ij} is calculated as a function of the volume-conserving stress that breaks the symmetry. Reference [24] provides more information about the accounts. Using the following expression, the internal strain parameter (ζ) can be calculated:

$$\xi = \frac{C_{11} + 8C_{12}}{7C_{11} + 2C_{12}} \tag{4}$$

The upper limit of (ζ) corresponds to the insignificant contribution of the bond stretching/contracting to resist external stress., while the lower limit represents the insignificant contribution of the bond bending to resist the external stress. For crystalline solids of cubic shape, there are three types of independent elastic constants (C_{11}, C_{22} and C_{44}) that are used to check the mechanical stability according to Born criteria such as given in equation (5).

$$C_{11} - C_{12} > 0;\ C_{11} + 2C_{12} > 0;\ C_{11} > 0;\text{and } C_{44} > 0 \tag{5}$$

Table (3) The computed elastic constants for $BiGaO_3$ display that the unidirectional elastic consistent C_{11}, that's associated with unidirectional strain alongside the main crystal direction, is a good deal better than C_{44}, which suggests that $BiGaO_3$ has a weaker resistance to pure shear deformation as compared to the unidirectional compressive resistance. In a cubic crystal, there are conditions for the classical mechanical stability of elastic constants. The estimated elastic constants in table (3) satisfied the above-mentioned stability conditions, suggesting that $BiGaO_3$ is mechanically stable. After evaluating the elastic constants ($C_{11}, C_{22},$ and C_{44}) for $BiGaO_3$, we can estimate relevant properties such as shear modulus (G), bulk modulus B, Poisson's ratio (ν), Young's modulus (E), Lame's coefficients (μ,λ), and Pugh ratio (G/B) [25-27] by using the following relations:

$$G = \frac{G_V + G_R}{2} \tag{6}$$

$$C_V = \frac{C_{11} - C_{12} + 3C_{44}}{5} \tag{7}$$

$$C_R = \frac{5(C_{11} - C_{12})C_{44}}{4C_{44} + 3(C_{11} - C_{12})} \tag{8}$$

$$\nu = \frac{3B+E}{6B} \tag{9}$$

$$E = \frac{9BG}{3B+G} \tag{10}$$

$$\mu = \frac{E}{2(1+\nu)} \tag{11}$$

$$\lambda = \frac{\nu E}{(1+\upsilon)(1-2\upsilon)} \tag{12}$$

Table (3) corresponds to the present value of the shear modulus and for the bulk modulus of $BiGaO_3$(B = 205.72 GPa and G = 104.32 GPa). Teter [28] illustrated that high values of shear modulus and bulk modulus are a guide and indicator of hardness. It is worthy to note that covalent and ionic bonds are distributed between cations that might be octahedral or cube-octahedral rounded by O atoms in $BiGaO_3$ compound [29]. The calculated results reveal that the nature $BiGaO_3$ compound is ionic, as the Poisson ratio calculated to be close to 0.3, and it was found that the calculated G/B value for $BiGaO_3$ is equal to (0.5), which also shows this compound bonding is of an ionic nature, where it can reveal (G/B) On the brittle or ductile behavior of the studied compound, it was shown from the ratio (G/B) that it has a strong ductile character [30,31]. The strong ductile character and ionic properties observed for $BiGaO_3$ compound indicate its suitability for practical device applications.

Table3. Calculated elastic parameters C_{ij}(GPa),Young's modulus E(GPa),shear modulus G (GPa),bulk modulus B(GPa),Pugh'sindex G/B, Poisson's ratio(υ) internal strain parameter (ζ), anisotropy factor A,and Lame's coefficients (μ,λ) of$BiGaO_3$.

parameter	C_{11}	C_{12}	C_{44}	E	G	B	G/B	ν	ζ	A	λ	μ
this work	364	126	95	269	105	205	0.5	0.28	0.49	0.8	134	105
Ref[32]	387.7	128.9	119	309.9	123	215.1	0.57	0.74	0.48	0.92	274.5	89
Ref[33]	375.8	129.7	98.3	267.7	104.3	205.7	0.51	0.28	0.5	0.86	136.7	103.3

4. Conclusion

The GGA-PBE approximation was used to calculate the optical properties, electronic structures, elastic constants, and the structural parameters of $BiGaO_3$. The computed lattice constants of $BiGaO_3$ agree with other theoretical results. The calculated crystal structure of $BiGaO_3$ indicates that it possesses a cubic crystal structure with a space group pm-3m(221#). Moreover, the electronic structures revealed that the upper part of the valence bands were identified by the O-2p states, and the lower part of the conduction bands were identified by the Bi-6p states. Electronic structure calculations showed that $BiGaO_3$ is a semiconductor with an indirect M-X band gap separating the conduction bands (CB) from the valence bands (VB). The value of the calculated elastic constants for C_{ij} is positive, indicating that $BiGaO_3$ is characterized by mechanical stability.

The current results assume the character of ionic bonding of the studied compound and lead to be ductile material classified. The real and imaginary parts of the dielectric functions, extinction coefficient, refractive index, reflectivity spectra, electronic energy loss function, optical absorption coefficient, real part of the optical and optical conductivity of the composite were determined. It is observed that $n(\omega)$ and $k(\omega)$ have almost the same properties as $\varepsilon_1(\omega)$ and $\varepsilon_2(\omega)$, respectively, $BiGaO_3$ has interesting as piezoelectric, ferroelectric, multiferroic, and photo catalytic materials.

References

[1] Zubko, P., Gariglio, S., Gabay, M., Ghosez, P., &Triscone, J. M. (2011). Interface physics in complex oxide heterostructures. Annu. Rev. Condens. Matter Phys., 2(1), 141-165; https://doi.org/10.1146/annurev-conmatphys-062910-140445

[2]Kimura, T., Goto, T., Shintani, H., Ishizaka, K., Arima, T. H., &Tokura, Y. (2003). Magnetic control of ferroelectric polarization. nature, 426(6962), 55-58.

[3] Cheong, S. W., &Mostovoy, M. (2007). Multiferroics: a magnetic twist for ferroelectricity. Nature materials, 6(1), 13-20; https://doi.org/10.1038/nmat1804

[4] Belik, A. A. (2012). Polar and nonpolar phases of $BiMO_3$: a review. Journal of Solid State Chemistry, 195, 32-40; https://doi.org/10.1016/j.jssc.2012.01.025

[5] Baettig, P., Schelle, C. F., LeSar, R., Waghmare, U. V., &Spaldin, N. A. (2005). Theoretical prediction of new high-performance lead-free piezoelectrics. Chemistry of materials, 17(6), 1376-1380; https://doi.org/10.1021/cm0480418

[6] Inaguma, Y., Miyaguchi, A., Yoshida, M., Katsumata, T., Shimojo, Y., Wang, R., &Sekiya, T. (2004). High-pressure synthesis and ferroelectric properties in perovskite-type $BiScO_3$-$PbTiO_3$ solid solution. Journal of applied physics, 95(1), 231-235; https://doi.org/10.1063/1.1629394

[7] Belik, A. A., Wuernisha, T., Kamiyama, T., Mori, K., Maie, M., Nagai, T., ...&Takayama-Muromachi, E. (2006). High-pressure synthesis, crystal structures, and properties of perovskite-like BiAlO3 and pyroxene-like $BiGaO_3$. Chemistry of materials, 18(1), 133-139; https://doi.org/10.1021/cm052020b

[8] Zhang, J. Z., Ding, H. C., Zhu, J. J., Li, Y. W., Hu, Z. G., Duan, C. G., ... & Chu, J. H. (2014). Electronic structure and optical responses of nanocrystalline $BiGaO_3$ films: A combination study of experiment and theory. Journal of Applied Physics, 115(8), 083110; https://doi.org/10.1063/1.4867006

[9] Belik, A. A., Stefanovich, S. Y., Lazoryak, B. I., &Takayama-Muromachi, E. (2006). $BiInO_3$: a polar oxide with $GdFeO_3$-type perovskite structure. Chemistry of materials, 18(7), 1964-1968; https://doi.org/10.1021/cm052627s

[10] Wang, H., Wang, B., Li, Q., Zhu, Z., Wang, R., & Woo, C. H. (2007). First-principles study of the cubic perovskites Bi M O_3 (M= Al, Ga, In, and Sc). Physical Review B, 75(24), 245209; https://doi.org/10.1103/PhysRevB.75.245209

[11]Wang, H., Wang, B., Wang, R., & Li, Q. (2007). Ab initio study of structural and electronic properties of $BiAlO_3$ and $BiGaO_3$. Physica B: Condensed Matter, 390(1-2), 96-100; https://doi.org/10.1016/j.physb.2006.07.070

[12]Kohn, W., & Sham, L. J. (1965). Self-consistent equations including exchange and correlation effects. Physical review, 140(4A), A1133; https://doi.org/10.1103/PhysRev.140.A1133

[13]Perdew, J. P., Chevary, J. A., Vosko, S. H., Jackson, K. A., Pederson, M. R., Singh, D. J., &Fiolhais, C. (1992). Atoms, molecules, solids, and surfaces: Applications of the generalized gradient approximation for exchange and correlation. Physical review B, 46(11), 6671; https://doi.org/10.1103/PhysRevB.46.6671

[14]Perdew, J. P., Burke, K., &Ernzerhof, M. (1996). Generalized gradient approximation made simple. Physical review letters, 77(18), 3865; https://doi.org/10.1103/PhysRevLett.77.3865

[15] Ghaleb, A. M., Munef, R. A., & Mohammed, S. F. (2022). First principles study the effect of Zn doped MgO on the energy band gap using GGA approximation. *Journal of Ovonic Research*, *18*(1) ; https://doi.org/10.15251/JOR.2022.181.11

[16]Hilal, M., Rashid, B., Khan, S. H., & Khan, A. (2016). Investigation of electro-optical properties of InSb under the influence of spin-orbit interaction at room temperature. Materials Chemistry and Physics, 184, 41-48; https://doi.org/10.1016/j.matchemphys.2016.09.009

[17]Sahin, S., Ciftci, Y. O., Colakoglu, K., &Korozlu, N. (2012). First principles studies of elastic, electronic and optical properties of chalcopyrite semiconductor $ZnSnP_2$. Journal of alloys and compounds, 529, 1-7; https://doi.org/10.1016/j.jallcom.2012.03.046

[18]Zhang, J. Z., Ding, H. C., Zhu, J. J., Li, Y. W., Hu, Z. G., Duan, C. G., ... & Chu, J. H. (2014). Electronic structure and optical responses of nanocrystalline $BiGaO_3$ films: A combination study of experiment and theory. Journal of Applied Physics, 115(8), 083110; https://doi.org/10.1063/1.4867006

[19]Murtaza, G., Khenata, R., Mohammad, S., Naeem, S., Khalid, M. N., &Manzar, A. (2013). Structural, elastic, electronic and optical properties of $CsMCl_3$ (M= Zn, Cd). Physica B: Condensed Matter, 420, 15-23; https://doi.org/10.1016/j.physb.2013.03.011

[20]Xu, B., Li, X., Sun, J., & Yi, L. (2008). Electronic structure, ferroelectricity and optical properties of $CaBi_2Ta_2O_9$. The European Physical Journal B, 66(4), 483-487; https://doi.org/10.1140/epjb/e2008-00461-9

[21]Li, L., Wang, W., Liu, H., Liu, X., Song, Q., &Ren, S. (2009). First principles calculations of electronic band structure and optical properties of Cr-doped ZnO. The Journal of Physical

Chemistry C, 113(19), 8460-8464; https://doi.org/10.1021/jp811507r

[22]Schreiber, E., Anderson, O. L., Soga, N., & Bell, J. F. (1975). Elastic constants and their measurement; https://doi.org/10.1115/1.3423687

[23] Ghaleb, A. M., & Ahmed, A. Q. (2022). Structural, electronic, and optical properties of sphalerite ZnS compounds calculated using density functional theory (DFT). *Chalcogenide Letters*, *19*(5);https://doi.org/10.15251/CL.2022.195.309

[24]Mehl, M. J. (1993). Pressure dependence of the elastic moduli in aluminum-rich Al-Li compounds. Physical Review B, 47(5), 2493; https://doi.org/10.1103/PhysRevB.47.2493

[25]Bouhemadou, A., Khenata, R., Kharoubi, M., Seddik, T., Reshak, A. H., & Al-Douri, Y. (2009). FP-APW+ lo calculations of the elastic properties in zinc-blende III-P compounds under pressure effects. Computational materials science, 45(2), 474-479; https://doi.org/10.1016/j.commatsci.2008.11.013

[26]Tvergaard, V., & Hutchinson, J. W. (1988). Microcracking in ceramics induced by thermal expansion or elastic anisotropy. Journal of the American Ceramic Society, 71(3), 157-166; https://doi.org/10.1111/j.1151-2916.1988.tb05022.x

[27]Pugh, S. F. (1954). XCII. Relations between the elastic moduli and the plastic properties of polycrystalline pure metals. The London, Edinburgh, and Dublin Philosophical Magazine and Journal of Science, 45(367), 823-843; https://doi.org/10.1080/14786440808520496

[28]Teter, D. M. (1998). Computational alchemy: the search for new super hard materials. MRS bulletin, 23(1), 22-27; https://doi.org/10.1557/S0883769400031420

[29]Alay-e-Abbas, S. M., Nazir, S., Noor, N. A., Amin, N., &Shaukat, A. (2014). Thermodynamic stability and vacancy defect formation energies in $SrHfO_3$. The Journal of Physical Chemistry C, 118(34), 19625-19634; https://doi.org/10.1021/jp506263g

[30]Kanoun, M. B., Merad, A. E., Cibert, J., Aourag, H., &Merad, G. (2004). Propertiesofstrainedzinc-blendeGaN: first-principlesstudy. Journal of alloys and compounds, 366(1-2), 86-93; https://doi.org/10.1016/j.jallcom.2003.07.005

[31] Frantsevich, I. N. (1982). Elastic constants and elastic moduli of metals and insulators. Reference book.

[32]Tse, G., &Yua, D. (2015) .The first principle study electronic and optical properties in $BiGaO_3$; Asian Journal of Current Engineering and Maths 4:5, September - October ,pp 56 – 61; http:// doi.org/10.15520/ajcem.

[33] Kourdassi, A., Benkhettou, N., Labair, M., Benkabou, M., Benalia, S., Khenata, R., ...&Rached, D. (2014). FP-LMTO calculations of the structural, elastic, thermodynamic, and electronic properties of the ideal-cubic perovskite $BiGaO_3$. Brazilian Journal of Physics, 44(6), 914-921; https://doi.org/10.1007/s13538-014-0262-2